CHEMISTRY

AN ASIAN JOURNAL

www.chemasianj.org

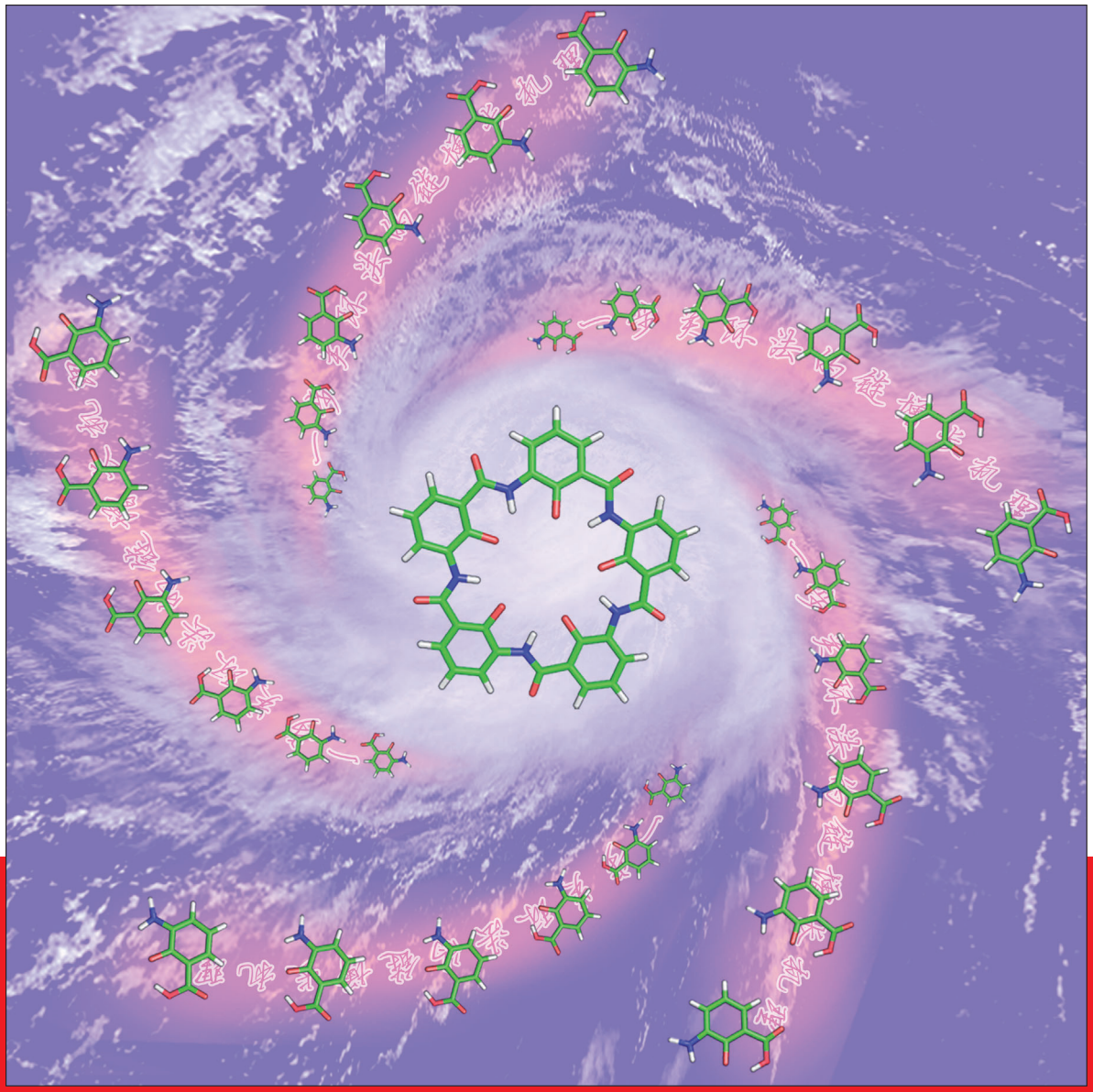

12/06
2011

IYC 2011
International Year of CHEMISTRY

One-pot hydrogen-bonding-assisted macrocyclizations …

… have received considerable recent interest due to their already proven and other potentially realizable functions and applications. Mechanistic investigations on one-pot macrocyclizations, however, are scarce. In their Full Paper on page 3298 ff, H. Q. Zeng et al. demonstrate, for the first time, the applicability of a chain-growth mechanism to the $POCl_3$-mediated one-pot macrocyclization reaction, allowing for the highly selective formation of five-residue macrocycles formed by the successive addition of bifunctional monomer units onto the growing oligomeric backbone.

An ACES journal

Supported by:
GDCh Gesellschaft Deutscher Chemiker
ChemPubSoc Europe

WILEY-VCH

Inside Cover

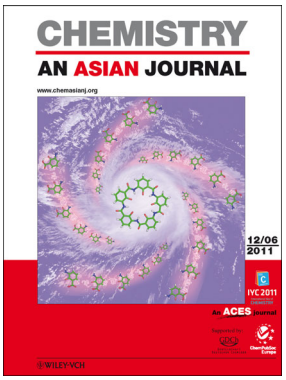

Bo Qin, Sheng Shen, Chang Sun, Zhiyun Du, Kun Zhang, and Huaqiang Zeng*

One-pot hydrogen-bonding-assisted macrocyclizations …

… have received considerable recent interest due to their already proven and other potentially realizable functions and applications. Mechanistic investigations on one-pot macrocyclizations, however, are scarce. In their Full Paper on page 3298 ff, H. Q. Zeng et al. demonstrate, for the first time, the applicability of a chain-growth mechanism to the $POCl_3$-mediated one-pot macrocyclization reaction, allowing for the highly selective formation of five-residue macrocycles formed by the successive addition of bifunctional monomer units onto the growing oligomeric backbone.

DOI: 10.1002/asia.201100409

One-Pot Multimolecular Macrocyclization for the Expedient Synthesis of Macrocyclic Aromatic Pentamers by a Chain Growth Mechanism

Bo Qin,[a] Sheng Shen,[a] Chang Sun,[a] Zhiyun Du,[b] Kun Zhang,[b] and Huaqiang Zeng*[a]

Abstract: $POCl_3$-mediated one-pot macrocyclization allows the highly selective formation of five-residue macrocycles that are rigidified by internally placed intramolecular hydrogen bonds. Mechanistic investigation by using tailored competition experiments and kinetic simulation provides a comprehensive model, supporting a chain-growth mechanism underlying the one-pot formation of aromatic pentamers, whereby the successive addition of a bifunctional monomer unit onto either another monomer or the growing oligomeric backbone is faster than other types of bimolecular condensations involving oligomers longer than monomers. DFT calculations at the B3LYP/6-31G* level reveal the five-residue pentamer to be the most stable with respect to alternative four-, six-, and seven-residue macrocycles. These novel mechanistic insights may become useful in analyzing other macrocyclization, oligomerization, and ploymerization reactions.

Keywords: foldamers · hydrogen bonds · macrocycles · macrocyclization mechanism · supramolecular chemistry

Introduction

Since the seminal works on macrocyclic ligands by Pedersen,[1a,b] Lehn,[1c,d] and Cram,[1e,f] macrocyclic chemistry has prospered over the past four ensuring decades to become one of the most dynamic and promising frontiers of chemical research. Researching and identifying new macrocyclic molecules with novel properties have therefore continuously attracted multidisciplinary interests. Efficient construction of macrocyclic backbones to derive a "macrocyclic effect", however, has been a constant challenge. To promote the effective macrocyclization, one-step cyclization, templated cyclization, intramolecular ring closure, intermolecular coupling, dynamic covalent bond formation, and conformation-assisted macrocyclization have been developed.[2–3] Despite these intensive efforts and synthetic advancements, most of the cyclization reactions are still carried out under conditions of high dilution, and critical challenges remain in the efficient construction of functional macrocycles with precise control over the ring sizes and the variable functionalization around the periphery.[2] As a recently emerging concept, the one-pot hydrogen-bonding-assisted macrocyclization strategy is among the newest, arguably the most efficient addition to the macrocyclization toolbox.[3c,4] This strategy currently is very limited in substrate scope and applicable to only a few monomer building blocks. Moreover, mechanistic investigation on one-pot macrocyclization[2–3,4a–j] has been very scarce with only one recent report by Gong[4e] that is known to us.

To further expand the structural diversity of macrocycles, their already demonstrated diverse functions,[4f,5] and other potentially realizable functions and applications,[4k,6a] we recently reported our work on the use of $POCl_3$ as a powerful cyclization agent to promote one-pot hydrogen-bonding-assisted macropentamerization that allows efficient highly selective preparation of a series of circularly folded pentamers, such as **1**, under mild conditions.[4k] In other words, the one-pot macrocyclization protocol enables precise control over the ring size of formed macrocycles that are characterized by an intrinsic backbone propensity that requires five repeating units to form a macrocycle[4k,l,5e,6a] or a helical turn.[6b,c] Our very recent continuing exploration further reveals that the $POCl_3$-mediated one-pot macrocyclization also leads to the variable functionalizations around the pentameric periphery.[4l] More specifically, a hybrid macrocycle, such as **3**, can be conveniently prepared as the major prod-

[a] B. Qin, S. Shen, C. Sun, Dr. H. Q. Zeng
Department of Chemistry
National University of Singapore
3 Science Drive 3, Singapore, 117543 (Singapore)
Fax: (+65) 6779-1691
E-mail: chmzh@nus.edu.sg

[b] Dr. Z. Y. Du, Prof. Dr. K. Zhang
Faculty of Chemical Engineering and Light Industry
Guang Dong University of Technology
Guang Dong, 510006 (China)

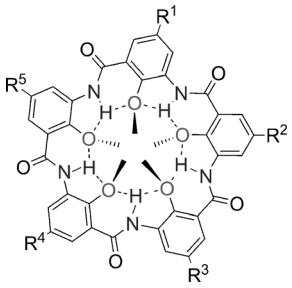

1: $R^1 = R^2 = R^3 = R^4 = R^5 = H$
2: $R^1 = R^2 = R^3 = R^4 = R^5 = OC_8H_{17}$
3a: $R^1 = R^2 = R^3 = OC_8H_{17}$, $R^4 = R^5 = H$
3b: $R^1 = R^2 = OC_8H_{17}$, $R^3 = R^4 = R^5 = H$
3c: $R^1 = OC_8H_{17}$, $R^2 = R^3 = R^4 = R^5 = H$

uct through one-pot comacrocyclization of two different monomers that differ by their exterior side chains. This finding differs from those outstanding works on the hybird 3D-shaped macrocycles previously reported by Huang that were produced more or less statistically.[7] We postulated that the $POCl_3$-mediated one-pot macrocyclization proceeds predominantly by a chain-growth mechanism in which the addition of monomer into the growing backbones (n+1-type reaction, Scheme 1) is faster than other competing bimolecular reactions between two monomers or between two higher oligomers.[4l] In other words, the inequality 1 [Eq. (1)] should hold qualitatively:

$$K_{1+1},\ K_{2+2},\ \text{or}\ K_{3+2} < K_{n+1}\ (n = 2-4) \qquad (1)$$

In the present study, we provide convincing evidence and detailed analyses that support a stepwise chain-growth mechanism underlying the preferred formation of five-residue aromatic pentamers by one-pot macrocyclization with an in-depth understanding of the reaction mechanism going beyond that contained within inequality 1 [Eq. (1)]. This was achieved by carrying out tailored competition experiments and performing kinetic simulations by using experimental yields. Additionally, a low to undetectable experimental occurrence of four-, six-, and seven-residue macrocycles can be explained computationally on the basis of the relative energy per repeating unit that becomes increasingly more stable in the order of tetramer < heptamer < hexamer < pentamer.

Results and Discussion

As discussed above, the $POCl_3$-mediated one-pot macrocyclization reaction now allows an efficient preparation of aromatic pentamers carrying side chains of varying types in both its interior[4k] and exterior.[4l] This efficient macrocylization stems from the persistent folding of backbone into a crescent-shaped conformation induced by internally located continuous hydrogen-bonding forces as demonstrated by us.[5e,6] At the start of the macrocylization reaction, intermolecular reactions dominate and result in the formation of intermediate oligomers with a hydrogen-bonding-enforced curved backbone. As sketched in Scheme 1, the oligomers of suitable lengths, such as a dimer and a trimer may undergo bimolecular 2+3-type cyclization reactions to produce aromatic pentamers. The over-shooting products, such as hexamers, are minimized owing to the remote steric hindrance. This mechanism was demonstrated to be operational during the highly efficient preparation of macrocycles containing even numbers of symmetrical bifunctional monomers through one-pot multimolecular macrocylization.[4e] Is this mechanism equally applicable to the presently studied aromatic pentamers consisting of unsymmetrial bifunctional building blocks?

Alternatively, the incorporation of additional building blocks into short intermediate oligomers by a chain-growth mechanism (Scheme 1) eventually should lead to an acyclic pentamer precursor, the increasingly curved backbone of which brings two reactive sites at its two ends into a close proximity to facilitate an intramolecular cyclization, thus producing aromatic pentamers. This simplified scenerio leaves us a few outstanding questions: 1) How are the acyclic pentamer precursors produced? 2) What are their relative reaction rates? 3) Is there any rate-determining step during the chain-extension process? 4) How are the under- or over-shooting macrocycles and other acyclic oligomers minimized, giving rise to the preferred formation of pentagon-shaped five-residue macrocycles? As the formation of a circular hexamer is very minimal and no circular tetramer has been experimentally observed,[4k] the current mechanistic investigation will mainly focus on the desired pathways that lead to the formation of circular pentamers.

Competition Experiments for Mechanistic Elucidation

Our previous data obtained only provided very preliminary insights into the chain-growth mechanism underlying one-pot macrocyclization.[4l] To further confirm this hypothetical mechanism, a new set of competition experiments has to be and was designed that involves monomer **2a**, dimer **1a**, and trimer **1b** in various ratios, affording reaction mixtures containing up to five circular pentamers **1**, **2**, **3a**, **3b**, and **3c** with their isolated chemical yields tabulated in Table 1 and TLC-mediated separation illustrated in Figure 1.

A few useful conclusions can be drawn from the presently designed competition experiment involving **1a**, **1b**, and **2a**. 1) Given $K_{4+1} > K_{2+3}$ from inequality 1 [Eq. (1)], it can be concluded from entry 1 of Table 1 that K_{2+2} is much slower than K_{3+2}; otherwise, with respect to **1**, pentamer **3c** should be produced in >24% yield,[8b] a yield much higher than 14% (Table 1, entry 1), by combining a two-step process (e.g, by a K_{2+2} reaction involving dimer **1a**, producing a

Abstract in Chinese:

摘要：我们研究小组在近期的研究工作中报道了一种由 $POCl_3$ 诱导的一步关环法去实现选择性的合成芳香五元环折叠体。这种大环折叠体由五个单体组成，其骨架构象由氢键锁定。本文详细研究了由 $POCl_3$ 诱导的一步关环法的机理。我们发现链增长机理可以有效的解释五元环折叠体的产生过程。在这种链增长机理中，单体间或单体与寡聚体间的反应速率要比寡聚体间的快。此种新颖的链增长机理的获得对其他类性的大环关环，寡聚化 和聚合反应的机理研究必将有一定的帮助。

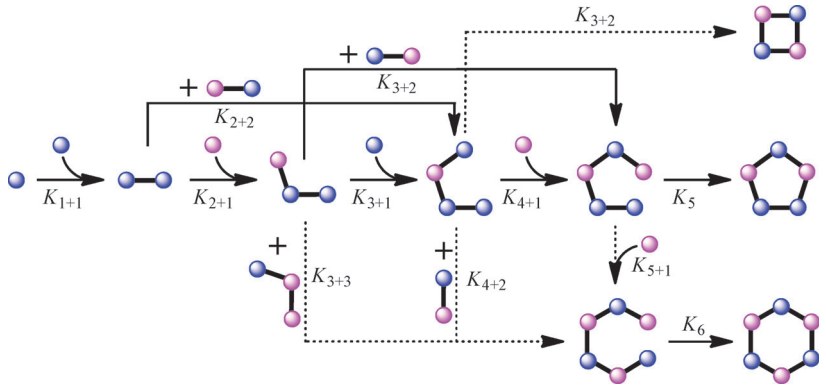

Scheme 1. Possible reaction pathways accounting for the preferred formation of acyclic pentamers—precursors for circular aromatic pentamers. The circular aromatic tetramers (under-shooting products) and hexamers (over-shooting products) may be formed from the reaction. Due to the steric hindrance and possible differences in thermodynamic stability of oligomer intermediates, some bimolecular reactions may be faster than the others. These relative reaction rates determine the mechanistic pathways underlying the one-pot macrocyclization. The balls in blue or purple represent the identical repeating units or those that differ by their exterior side chains. K is the reaction rate and $K_{n+m}=K_{m+n}$.

Table 1. Chemical yields[8a] for the one-pot preparation[a,b] of circular pentamers **1**–**3** from the corresponding oligomers **1a**, **1b**, and **2a**.

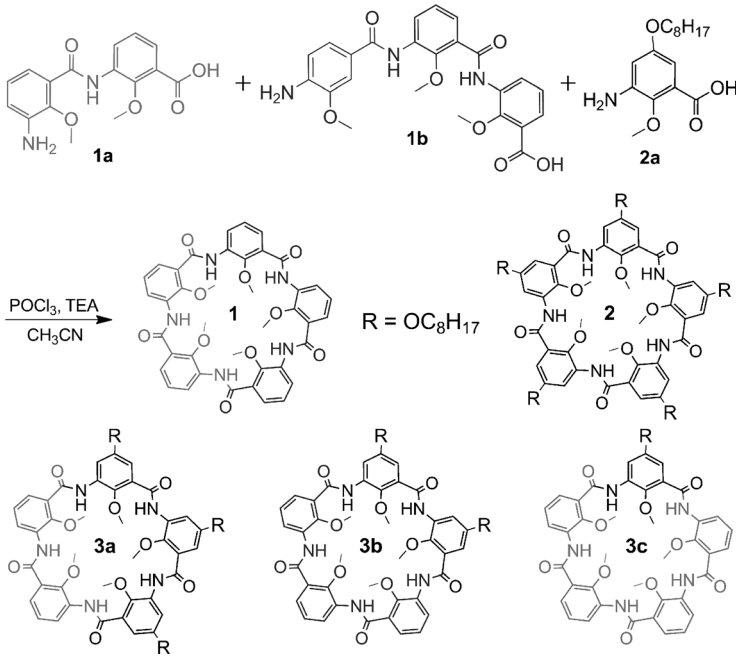

Entry	Reacting partners (**1a**/**1b**/**2a**)	Product distribution patterns and yields [%][a]				
		1	**2**	**3a**	**3b**	**3c**
1	1:1:1	41±2	trace	8±1	18±1	14±2
2	1:1:2	26±3	6±2	12±1	25±2	13±2
3	1:1:3	18±3	12±2	14±2	24±3	12±1
4	1:1:4	12±4	10±2	21±2	32±2	10±1
5	1:1:5	6±1	11±1	25±2	31±1	4±1

[a] Isolated yield by preparative TLC plates and averaged over a triplicate run. [b] Reaction conditions: reactants **1a**, **1b**, and **2a** (total = 0.2 mmol), $POCl_3$ (0.4 mmol), TEA (0.6 mmol), CH_3CN (2.0 mL), room temperature, 12 h.

tetramer that subsequently reacts with **2a** by a K_{4+1} reaction) with the K_{2+3} reaction involving dimer **1a** and in situ-generated trimer. 2) As discussed above, K_{1+1} may be slower than K_{n+1} ($n>1$); nevertheless, its value shall be quite similar to K_{n+1} as inferred from entry 3 of Table 1 in which pentamer **2** was produced with a K_{1+1} reaction as the first step and with a 12% yield that compares very favorably with a 14% yield for **3a**. While the differential rate constants between K_{1+1} and K_{2+3} cannot be confidently deduced from these competition experiments, the discussion from the succeeding section on kinetic simulations does suggest that the K_{1+1} reaction may be faster than the K_{3+2} reaction. 3) Although K_{4+1} possibly can be a low-yielding step (~50% from the above discussion), its reaction rate, however, shall be quite similar to K_5 and other K_{n+1} ($n=2$ and 3) reactions. The support for this comes from the fact that the production of pentamer **3a** by a four-step coupling process is about 50–80% of that of **3b** by a shorter three-step coupling process (Table 1, entries 1–5). If one of the coupling reactions involving K_5 and K_{n+1} ($n=2$–4) is significantly much slower than all the others, a comparable yield for producing **3a** and **3b** is expected. Indeed, in the absence of other closely related competing parties, pentamers **1**, **3a**, **3b**, and **3c** are produced in similar yields of 46,[4k] 38,[4l] 42,[4l] and 39%,[4l] respectively. Additionally, both the dimer and tetramer shall be present in substantial amounts during the 1+2+3-type reaction in which monomer, dimer, and trimer couples with each other to produce different pentamers (Table 1, entries 1–5), which, however, does not give rise to a hexamer. This suggests that the K_{4+2} reaction is slower than either K_{3+2}, K_{n+1} ($n=$ 1–4), or K_5. On this basis, inequality 2 [Eq. (2)] can be derived:

$$K_{2+2} \text{ or } K_{4+2} < K_{3+2} < K_{1+1} < K_{n+1} \approx K_5 \quad (n = 2-4) \tag{2}$$

Similar to pentamer **1**, we believe that **3c** was also formed by the K_{2+3} reaction involving dimer **1a** and in situ produced trimer that was produced by the K_{2+1} reaction between **1a** and **2a**. With increasing amounts of monomer **2a** (Table 1, entries 3–5), both the trimer intermediate and dimer **1a** were rapidly converted into tetramer and trimer by the respective faster K_{3+1} and K_{2+1} reactions, thus diminishing the K_{3+2} reaction to a negligible extent. The reasoning that pentamer **3c** is produced firstly by a K_{2+2} reaction involving dimer **1a**, producing a tetramer intermediate

CHEMISTRY
AN ASIAN JOURNAL

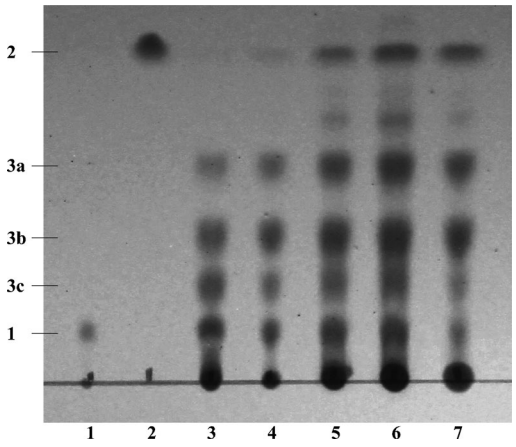

Figure 1. Product distributions illustrated by TLC analysis that involve pentamers **1**–**3** produced from the reactions specified in Table 1. Lane 1 = pentamer **1** containing no exterior side chains, Lane 2 = pentamer **2** containing five exterior octyoxy side chains, Lanes 3–7 = macrocylization reaction products generated by reacting **1a**, **1b**, and **2a** in molar ratios of 1:1:1, 1:1:2, 1:1:3, 1:1:4, and 1:1:5, respectively. Eluent: ethyl acetate/hexane = 1:3 (v/v). Note that the dark spots at the origin line actually derive from very tiny amounts of unknown compounds from the reaction.

that subsequently reacts with monomer **2a** by a K_{4+1} reaction is not supported by inequality 2 [Eq. (2)].

To additionally differentiate the reaction rates between K_{2+2} and K_{4+2}, another competition experiment was undertaken, involving a 1:1 mixture of tetramer **1c** containing no exterior side chains and dimer **2b** containing two exterior octyloxy side chains (Scheme 2). Experimentally, only a single type of hexamer **4a** containing two octyloxy-containing repeating units was formed in 25% yield, implying that K_{2+2} is significantly much slower than K_{4+2}. If K_{2+2} is comparable to or faster than K_{4+2}, a tetramer containing four octyloxy-containing units in situ generated by a K_{2+2} reaction would be produced that competes with tetramer **1c** in

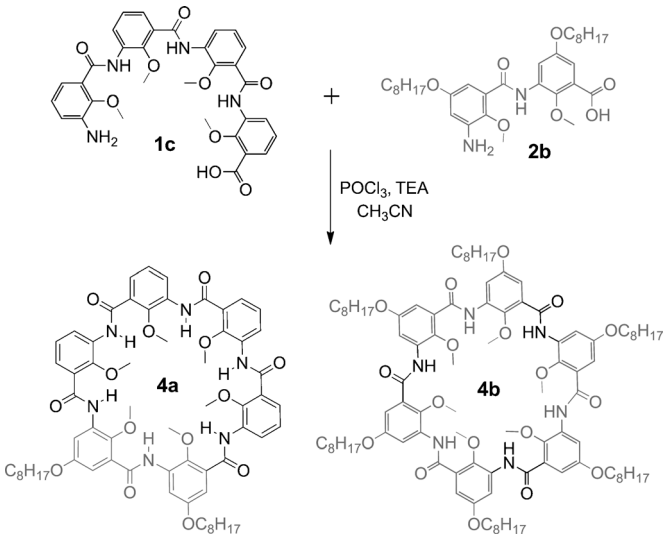

Scheme 2. Formation of hexamers **4a** and **4b**.

the reaction with dimer **2b** to produce a second type of hexamer **4b** containing six octyloxy-containing repeating units in it (see inequality 3 [Eq. (3)]).

$$K_{2+2} < K_{4+2} < K_{3+2} < K_{1+1} < K_{n+1} \approx K_5 \ (n = 2-4) \qquad (3)$$

Kinetic Simulation of Reaction Rates

The dependability of certain components in inequality 3 [Eq. (3)] dictating the preferred formation of pentamers of varying types can be verified by applying kinetic simulations onto entries 1–5 in Table 1 by assuming a best-case scenario in which 1) the same type of K_{n+m} reaction has the same rate constant regardless of the identity of monomers and oligomers and 2) oligomers higher than pentamers are not formed from the reaction, which is true experimentally, to reduce the complexity of simulations. In the simulation, no assumption on the chain-growth process for forming various pentamers was made. Instead, monomers and oligomeric intermediates are not allowed to grow beyond pentamers by any bimolecular reaction (see the Experimental Section for equations used).

Based on the respective chemical yields (Table 1, entries 1–5), a total of 24 reactions using seven variable reaction rates of K_{n+m} ($2 \le n+m \le 5$) and K_5 types were performed (see the Experimental Section for equations used). Simulations evolved over 3600 seconds with a step length of 1 second. The longer sampling time ensured that all the simulated yields obtained on circular pentamers are the maximum yields possible under the stipulated set of kinetic rates with >99.9% formation of the respective pentamers that should have be produced. The convergent criteria were chosen in such a way that the simulated chemical yields shall fall within the experimental ranges. For instance, from entry 2 of Table 1, **2** was produced in 6±2% over a triplicate run; it would be considered as ideal if the simulated chemical yield of **2** falls within 4–8%, preferably equal to the average value of 6%. In addition, the rate constants obtained based on one entry ideally shall be applicable to other entries to cross-test the reliability of obtained values.

After going through iterations of numerous rounds by using kinetic simulators freely available online,[9a] the close to best-fit kinetic rate constants and the simulated chemical yields were obtained, compiled, and compared to experimental ones as shown in Table 2.

It was found that a slight increase or decrease in the value for K_{2+2} relative to K_{3+2} significantly influenced the simulated yields of both **1** and **3c** for entries 1 and 2 of Table 2, leading to larger deviations from experimental ranges. For instance, with respect to 1) $K_{2+2} = 0.002$ and 2) all the other rate constants remained unchanged, the simulated yields of **1** and **3c** for $K_{2+2} = 0$ increased from 39 and 15% to 46 and 17%, respectively. For $K_{2+2} = K_{3+2} = 0.008$, the simulated yields for **1** and **3c** decreased from 39 and 15% to 29 and 11%, respectively. With $K_{2+2} = 5 \times K_{3+2} = 0.04$, the simulated yields for **1** and **3c** further decreased to respective 14 and 8%. These comparisons are consistent with experimental

Table 2. Simulated rate constants for the bimolecular reactions used to model cyclopentamerization and the corresponding simulated chemical yields for circular pentamers **1**–**3** made from oligomers **1a**, **1b**, and **2a** as shown in Table 1.

Entry	Reacting partners	Simulated kinetic rate constants [s^{-1}][a]							Product distribution patterns + yields [%][b]				
	(**1a**/**1b**/**2a**)	K_{1+1}	K_{2+1}	K_{3+1}	K_{4+1}	K_{2+2}	K_{3+2}	K_5	**1**	**2**	**3a**	**3b**	**3c**
1	1:1:1	0.036	0.060	0.045	0.040	0.002	0.008	>0	39	2	5	11	15
									(0)	(−2)	(−2)	(−6)	(0)
2	1:1:2	0.036	0.060	0.045	0.040	0.002	0.008	>0	27	8	14	22	15
									(0)	(0)	(1)	(−1)	(0)
3	1:1:3	0.025	0.065	0.035	0.030	0.002	0.008	>0	17	12	20	25	12
									(0)	(0)	(4)	(0)	(0)
4	1:1:4	0.011	0.065	0.035	0.030	0.002	0.008	>0	7	11	23	30	7
									(−1)	(0)	(0)	(2)	(−2)
5	1:1:5	0.011	0.065	0.035	0.030	0.002	0.008	>0	5	15	27	34	5
									(0)	(3)	(0)	(2)	(0)

[a] Simulation over 3600 s that allows the respective yields to reach >99.9% of the maximum allowed chemical yields. [b] The values in brackets are the deviations of simulated yields from experimental ranges shown in Table 1; negative values = deviations from the lower boundary, positive values = deviations from the upper boundary, 0% = no derivations from the experimental ranges.

observations and our expectation that K_{2+2} shall be less than K_{3+2} so that, in the presence of a lesser amount of **2a** (Table 2, entry 1), K_{2+2} will not substantially compete with K_{3+2} to significantly decrease the yields for **1** and **3c**. Similarly, for entries 3–5 of Table 2, a slight difference in values of K_{n+1} (n=2–4) leads to larger deviations of the simulated chemical yields from experimental ones. Except for K_{1+1}, all the simulated K_{n+m} (n, $m \geq 1$) values do not vary significantly among entries 1–5 in Table 2, which delightedly allows the consistent reproduction of experimental trends in chemical yields shown in Table 1, though to a lesser degree for entry 1 in which the simulated yield derivates quite substantially for **3b**. From these simulated rate constants, the real rate constants are highly likely to increase in the order of $K_{2+2} < K_{3+2} < K_{1+1} < K_{3+1} \approx K_{4+1} < K_{2+1}$. This order nicely matches the qualitatively derived reactivity order shown in inequality 3 [Eq. (3)].

As K_5 corresponds to the intramolecular reaction that converts an acyclic pentamer into a circular one (Scheme 1), it is essentially a noncompeting reaction that does not compete with other reactions for reactants or intermediates of different types.[9b] With a sufficiently long enough reaction time, any positive value of K_5 in terms of reaction rate constant eventually transforms all the available acyclic pentamers into circular ones. As a result, its value cannot be confidently deduced on the basis of experimental yields (Table 2).

As exemplified by the obtained kinetic data for entry 4 of Table 2, Figure 2 illustrates simulated reaction progresses with the accumulated chemical yields for pentamers **1**–**3** plotted against the reaction time. The plateaus were reached at t=271, 212, 200, 86, and 300 seconds for **1**, **2**, **3a**, **3b**, and **3c**, respectively, which correspond to the 90% formation of these respective pentamers with their maximum allowable yields approaching 7.0, 10.8, 22.8, 29.7, and 6.6%. Within 1000–1100 seconds, all the pentamers reached 99.9% of their maximum allowable yields. In addition, all the starting oligomers **1a**, **1b**, and **2a** reached 90% consumption in about 50–60 seconds, and 99.9% consumption in about 800 seconds.

Ab Initio Molecular Modeling

The above analysis does not allow us to fully appreciate why 1) experimentally, circular hexamer was produced in a low yield of 6% during the one-pot preparation of pentamer **1**[4k] and 2) neither under-shooting tetramer nor over-shooting hepatmer were observed during the formation of aromatic pentam-

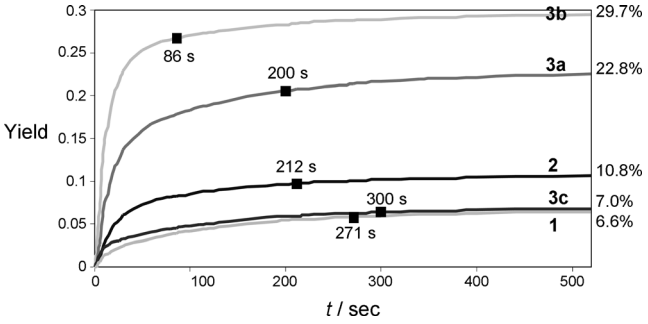

Figure 2. Kinetic simulation based on entry 4 of Table 1 on the formation and accumulation of circular pentamers **1**–**3** by one-pot macrocylization starting from bifunctional oligomers **1a**, **1b**, and **2a**. ■: refers to the time point at which 90% of the respective pentamers was produced from the cyclization reaction.

ers by one-pot condensation reactions. In other words, five-residue macrocycles form predominantly over other alternative macrocycles containing four, six, and seven repeating units. These, however, can be understood based on the plasticity of bond angles in the hydrogen-bonded backbone, allowing the backbone to curve toward the hydrogen-bonded side in responding to the hydrogen-bonding forces.[10] In the present system, the C−O···H−N hydrogen bonds were intentionally placed inside the interior to induce and to maintain a large curvature in the backbone that in turn results in a unique requirement, calling for five identical repeating units to furnish either a helical turn[6b,c] or a pentagon-shaped macrocycle.[5e,6a] Examination of crystal structures of circular pentamers[5e,6a] and helically folded pentamer and hexamer molecules[6b] demonstrates that the extent of backbone bending induced by internally placed hydrogen bonds is insignificantly influenced by macrocyclization constriction, necessitating an intrinsic need of five repeating units to form a regularly ordered helical or circular structure. This unique feature is also verifiable computationally[6] and is not seen in

other foldamer systems except for pentameric Schiff's base macrocycle recently reported.[11]

Theoretical treatments of circularly folded macrocycles containing from 4 to 7 residues provide the additional energetic details that help clarify the preferred formation of five-residue macrocycles over the other alternative sizes. By using DFT, macrocyclic foldamers of varying sizes in Figure 3 were optimized at the B3LYP/6-31G* level, followed by a single-point energy calculation at the B3LYP/6-311+G** level in the gas phase, CH_2Cl_2, and CH_3CN (Table 3). Among the four circular foldamers of varying sizes, pentamer **1** appears to be the most planar (Figure 3). As illustrated in entries 1, 3, and 4 from Table 3 and with respect to the gas phase, the incorporation of explicit solvents stabilizes the macrocyclic pentamers **5**–**7** by 3.14–3.77 and 3.79–4.39 kcal mol^{-1} in CH_2Cl_2 and CH_3CN, respectively, whereas the stability of pentamer **1** (Table 3, entry 2) surprisingly decreases by 4.28 and 3.63 kcal mol^{-1} in CH_2Cl_2 and CH_3CN, respectively. As a result, the values in relative energy among these four macrocyclic foldamers decrease from the gas phase to explicit solvents (Table 3, entries 5–8). For instance, pentamer **1** is more stable than **5**–**7** by at least 7.96 kcal mol^{-1} in the gas phase, whereas this value decreases to 0.50 kcal mol^{-1} in CH_2Cl_2. Despite of this, a general trend in terms of relative energy per repeating unit still persists among these four macrocycles in which the stability increases in the order of tetramer **5** < heptamer **7** < hexamer **6** < pentamer **1** with or without the consideration of explicit solvents. A difference of 0.52 kcal mol^{-1} per repeating unit between pentamer **1** and hexamer **6** in CH_3CN explains a low experimental occurrence of hexamer **6** (6% in CH_3CN[4k]). If the repeating units in hexamer **6** were used to construct pentamer **1**, the energetic destablization by these repeating units is estimated to be about 2.6 kcal mol^{-1} (5 × 0.52 kcal mol^{-1}) in CH_3CN. A relatively large difference of 4.56 or 1.00 kcal mol^{-1} per repeating unit between pentamer **1** and tetramer **5** or heptamer **6** in CH_3CN is consistent with the absence of both tetramer **5** and heptamer **6** from one-pot macrocyclization products involving starting oligomers of varying types in CH_3CN.[4k]

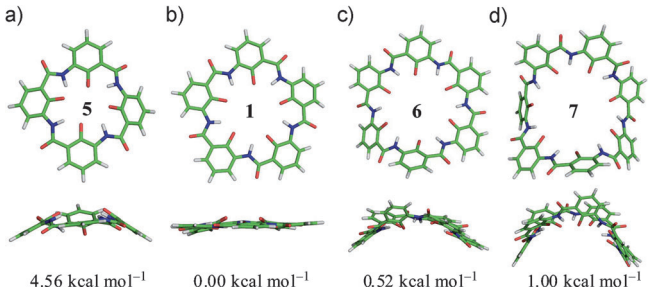

Figure 3. Top and side views of ab initio-optimized structures of circularly folded a) tetramer **5**, b) pentamer **1**, c) hexamer **6**, and d) heptamer **7** in acetonitrile at the B3LYP/6-31G* level. The computationally derived relative energy per repeating unit among these circular foldamers is normalized based on pentamer **1** in acetonitrile. The computationally derived planar backbone and geometry in **1** are nearly identical to those found in the crystal structure.[6a] For clarity of view, all the interior methyl groups in a–d) were removed.

Table 3. Computationally derived relative energy[a,b] per aromatic repeating unit among circularly folded aromatic macrocycles (**1** and **5**–**7**) in the gas phase, dichloromethane, and acetonitrile.

Entry	Circular aromatic foldamer	Relative energy per unit [kcal mol^{-1}]		
		gas phase	CH_2Cl_2	CH_3CN
1	circular tetramer **5**	**0.00**	−3.77	−4.39
2	circular pentamer **1**	**0.00**	4.28	3.63
3	circular hexamer **6**	**0.00**	−3.14	−3.79
4	circular heptamer **7**	**0.00**	−3.77	−4.39
5	circular tetramer **5**	12.52	4.54	4.56
6	circular pentamer **1**	**0.00**	**0.00**	**0.00**
7	circular hexamer **6**	7.96	0.50	0.52
8	circular heptamer **7**	9.03	1.09	1.00

[a] Density functional theory at the B3LYP/6-31G* level with the single-point energy calculated at the level of B3LYP/6-311+G**. [b] The relative energy per repeating unit from entries 1–4 and from entries 5–8 is normalized against gas-phase and pentamer **1**, respectively.

Conclusions

In concert with kinetic simulations, a competition experiment was carefully designed to facilitate the elucidation of mechanistic pathways as shown in Scheme 1 and corresponding relative reaction rates as expressed in inequalities 2 and 3 [Eq. (2) and (3)] and Table 2. Our findings present a clear support to the chain-growth process as the predominant mechanism, forming circular pentamers of varying types. Emphasizing the novel mechanistic insights for which the addition of monomer into the growing backbones is faster than other competing bimolecular reactions between two higher oligomers, this chain-growth mechanism differs from the one recently proposed by Gong that highlights the decisive roles of remote steric hindrance in the bimolecular reactions between two higher oligomers, producing suitably sized macrocycles.[4e] It is our belief that the chain-growth mechanism is operational for unsymmetrical bifunctional momomers, whereas Gong's mechanism is more suitable for symmetrical bifunctional momomers. Therefore, these two mechanisms fully complement each other and may offer insightful explanations to other macrocyclization, oligomerization, and polymerization scenarios involving (un)symmetrical bifunctional monomers as the repeating units.[2d]

Both experimentally and computationally, a necessity to have five repeating units per macrocycle is an intrinsic feature associated with the curved backbone stabilized by internally placed hydrogen bonds. This makes the pentamer the most stable among the four- to seven-residue macrocycles, thereby minimizing the production of under- and overshooting macrocycles.

Experimental Section

*One-pot preparation of pentamers **1–3**[12] from **1a**, **1b**, and **2a***

$POCl_3$ (38 μL, 0.4 mmol) was added to a solution of aromatic oligoamides **1a**, **1b**, and **2a** (total number of moles involving all the starting oligoamides is 0.2 mmol with the ratio **1a**/**1b**/**2a** ranging from 1:1:1 to 1:1:5) in CH_3CN (2.0 mL) at room temperature. The solution was vigorously stirred. After 10 min, Et_3N (84 uL, 0.6 mmol) was added into the reaction mixture. The solution was stirred for another 12 h, which was then concentrated in vacuo. The residue was purified by preparative TLC plates to afford circular pentamers **1**–**3**.

*One-pot preparation of hexamer **4a** from **1c** and **2b***

$POCl_3$ (38 uL, 0.4 mmol) was added to a solution of amino acid **1c** and **2b** (total number of moles involving the starting oligomers is 0.2 mmol, **1c**/**2b** = 1:1) in CH_3CN (2.0 mL) at room temperature. The solution was vigorously stirred. After 10 min, Et_3N (84 uL, 0.6 mmol) was added into the reaction mixture. The solution was stirred for 12 h and then concentrated in vacuo. The residue was purified by flash column chromatography (ethyl acetate/dichloromethane 1:10) to afford circular hexamer **4a** as a pale-yellow solid (29 mg, 25%). Decomposes at 205 °C; ^{1}H NMR (500 MHz, $CDCl_3$, 25 °C, TMS): δ = 9.76 (s, 1H; NH), 9.74 (s, 1H; NH), 9.73 (s, 1H; NH), 9.70 (s, 1H; NH), 9.67 (s, 1H; NH), 9.62 (s, 1H; NH), 8.80–8.70 (m, 4H; C_6H_6), 8.40 (d, $^3J_{H-H}$ = 3.2 Hz, 2H; C_6H_6), 7.99–7.91 (m, 4H; C_6H_6), 7.49–7.39 (m, 6H; C_6H_6), 4.08 (t, $^3J_{H-H}$ = 6.5 Hz, 4H; CH_2), 4.02 (s, 6H; OCH_3), 4.01 (s, 3H; OCH_3), 4.00 (s, 3H; OCH_3), 3.97 (s, 3H; OCH_3), 3.96 (s, 3H; OCH_3), 1.89–1.80 (m, 4H; CH_2 from C_8H_{17}), 1.55–1.45 (m, 4H; CH_2 from C_8H_{17}), 1.43–1.26 (m, 16H; CH_2 from C_8H_{17}), 0.92 ppm (t, $^3J_{H-H}$ = 6.9 Hz, 6H; CH_3 from C_8H_{17}). ^{13}C NMR (125 MHz, $CDCl_3$, 25 °C, TMS): δ = 163.41, 163.37, 163.34, 163.31, 156.38, 156.37, 147.68, 147.58, 147.55, 147.52, 141.18, 141.14, 132.58, 132.53, 131.91, 131.89, 131.88, 131.84, 127.24, 127.20, 127.16, 126.78, 126.70, 126.64, 126.61, 126.54, 126.37, 126.26, 125.95, 125.93, 125.91, 112.94, 112.85, 111.74, 111.58, 77.28, 77.03, 76.77, 68.73, 63.37, 63.36, 63.21, 63.19, 63.18, 31.83, 31.83, 29.33, 29.33, 29.25, 29.25, 29.19, 29.19, 26.01, 26.01, 22.68, 22.68, 14.12, 14.12 ppm; HRMS (EI): *m*/*z* (%): calcd for $C_{64}H_{74}N_6O_{14}$: 1173.5155 $[M+Na]^+$; found: 1173.5149.

Ab Initio Molecular Modeling

All the calculations were carried out by utilizing the Gaussian 03 program package.[13a] The geometry optimizations were performed at the DFT level, and the Becke's three parameter hybrid functional with the Lee–Yang–Parr correlation functional (B3LYP)[13b] method was employed to do the calculations. The 6-31G*[13c,d] basis from the Gaussian basis set library has been used in all the calculations. All the trimers and hexamers were relaxed fully without any symmetry constraints. The harmonic vibrational frequencies and zero-point energy corrections were calculated at the same level of theory. Single-point energies were obtained at the B3LYP level in conjunction with the 6-311+G (2d,p) basis set with the use of the above-optimized geometries, that is, B3LYP/6-311+G (2d,p)// B3LYP/6-31G (d).

Kinetic Simulations[9a] of K_{n+1} (n = 1–4), K_{2+2}, K_{2+3}, and K_5 as Shown in Scheme 1 and Table 2

Some assumptions were made: 1) Acyclic pentamers A5a–E5a are quantitatively converted into the corresponding circular pentamers A5b–E5b, which are largely true experimentally. 2) The same type of K_{n+m} reaction has the same rate constant regardless of the identity of monomers and oligomers. 3) Oligomers higher than pentamers are not formed from the reaction, which is true experimentally, to reduce the complexity of simulations. In the simulation, no assumption on the chain-growth process for forming various pentamers was made. Instead, monomers and oligomeric intermediates are allowed to grow not beyond pentamers by any bimolecular reaction. The following 24 equations were used in kinetic simulations in which An = Bn = Cn = Dn = En = oligomers containing n repeating units, A1 = acyclic monomer **2a**, A2 = B2 = acyclic dimer in which B2 = acyclic dimer **1a**, A3 = B3 = C3 = acyclic trimer in which C3 = acyclic trimer **1b**, A4 = B4 = C4 = acyclic tetramer, A5a = B5a = C5a = D5a = E5a = acyclic pentamer, and A5b = B5b = C5b = D5b = E5b = cyclic pentamers in which A5b = **2**, B5b = **3a**, C5b = **3b**, D5b = **3c**, and E5b = **1**.

K_{1+1} for A1 + A1 → A2
K_{1+2} for A1 + A2 → A3
K_{1+3} for A1 + A3 → A4
K_{2+2} for A2 + A2 → A4
K_{1+4} for A1 + A4 → A5a
K_{2+3} for A2 + A3 → A5a
K_5 for A5a → A5b = **2**

A1 = **2a**
Production of pentamer **2** (4)

K_{1+2} for A1 + B2 → B3
K_{1+3} for A1 + B3 → B4
K_{2+2} for A2 + B2 → B4
K_{1+4} for A1 + B4 → B5a
K_{2+3} for A2 + B3 → B5a
K_{2+3} for A3 + B2 → B5a
K_5 for B5a → B5b = **3a**

B2 = **1a**
Production of pentamer **3a** (5)

K_{1+3} for A1 + C3 → C4
K_{1+4} for A1 + C4 → C5a
K_{2+3} for A2 + C3 → C5a
K_5 for C5a → C5b = **3b**

C3 = **1b**
Production of pentamer **3b** (6)

K_{2+2} for B2 + B2 → D4
K_{1+4} for A1 + D4 → D5a
K_{2+3} for A2 + B3 → D5a
K_5 for D5a → D5b = **3c**

Production of pentamer **3c** (7)

K_{2+3} for B2 + C3 → E5a
K_5 for E5a → E5b = **1**

Production of pentamer **1** (8)

Acknowledgements

This work was financially supported by the NUS AcRF Tier 1 grants (R-143-000-375-112 & R-143-000-398-112 to H.Z.) and A*STAR BMRC research consortia (R-143-000-388-305 to H.Z.).

[1] a) C. J. Pedersen, *J. Am. Chem. Soc.* **1967**, *89*, 2415; b) C. J. Pedersen, *J. Am. Chem. Soc.* **1967**, *89*, 7017; c) B. Dietrich, J.-M. Lehn, J.-P. Sauvage, *Tetrahedron Lett.* **1969**, *10*, 2885; d) B. Dietrich, J.-M. Lehn, J.-P. Sauvage, *Tetrahedron Lett.* **1969**, *10*, 2889; e) E. P. Kyba, M. G. Siegel, L. R. Sousa, G. D. Y. Sogah, D. J. Cram, *J. Am. Chem. Soc.* **1973**, *95*, 2691; f) R. C. Helgeson, K. Koga, J. M. Timko, D. J. Cram, *J. Am. Chem. Soc.* **1973**, *95*, 3021.

[2] a) N. S. P. Knops, H. B. Mekelburger, F. Voegtle, *Top. Curr. Chem.* **1992**, *161*, 1; b) R. Faust, *Angew. Chem.* **1998**, *110*, 2985; *Angew. Chem. Int. Ed.* **1998**, *37*, 2825; c) S. Höger, *Chem. Eur. J.* **2004**, *10*, 1320; d) W. Zhang, J. S. Moore, *Angew. Chem.* **2006**, *118*, 4524; *Angew. Chem. Int. Ed.* **2006**, *45*, 4416.

[3] a) R. B. Woodward et al., *J. Am. Chem. Soc.* **1981**, *103*, 3213; b) A. Eschenmoser, *Angew. Chem.* **1988**, *100*, 5; *Angew. Chem. Int. Ed. Engl.* **1988**, *27*, 5; c) L. Y. Xing, U. Ziener, T. C. Sutherland, L. A. Cuccia, *Chem. Commun.* **2005**, 5751; d) F. Imabeppu, K. Katagiri, H. Masu, T. Kato, M. Tominaga, B. Therrien, H. Takayanagi, E. Kaji, K. Yamaguchi, H. Kagechika, I. Azumaya, *Tetrahedron Lett.* **2006**, *47*, 413; e) F. Campbell, J. Plante, C. Carruthers, M. J. Hardie, T. J. Prior, A. J. Wilson, *Chem. Commun.* **2007**, 2240; f) A. Yokoyama, T. Maruyama, K. Tagami, H. Masu, K. Katagiri, I. Azumaya, T.

Yokozawa, *Org. Lett.* **2008**, *10*, 3207; g) K. Katagiri, T. Tohaya, H. Masu, M. Tominaga, I. Azumaya, *J. Org. Chem.* **2009**, *74*, 2804; h) F. Campbell, A. J. Wilson, *Tetrahedron Lett.* **2009**, *50*, 2236; i) L. He, Y. An, L. Yuan, K. Yamato, W. Feng, O. Gerlitz, C. Zheng, B. Gong, *Chem. Commun.* **2005**, 3788; j) L. He, Y. An, L. H. Yuan, W. Feng, M. F. Li, D. C. Zhang, K. Yamato, C. Zheng, X. C. Zeng, B. Gong, *Proc. Natl. Acad. Sci. USA* **2006**, *103*, 10850; k) M. Geng, D. Zhang, X. Wu, L. He, B. Gong, *Org. Lett.* **2009**, *11*, 923.

[4] a) F. J. Carver, C. A. Hunter, R. J. Shannon, *Chem. Commun.* **1994**, 1277; b) L. Yuan, W. Feng, K. Yamato, A. R. Sanford, D. Xu, H. Guo, B. Gong, *J. Am. Chem. Soc.* **2004**, *126*, 11120; c) A. M. Zhang, Y. H. Han, K. Yamato, X. C. Zeng, B. Gong, *Org. Lett.* **2006**, *8*, 803; d) H. C. Ahn, S. M. Yun, K. Choi, *Chem. Lett.* **2008**, *37*, 10; e) W. Feng, K. Yamato, L. Q. Yang, J. S. Ferguson, L. J. Zhong, S. L. Zou, L. H. Yuan, X. C. Zeng, B. Gong, *J. Am. Chem. Soc.* **2009**, *131*, 2629; f) H. Jiang, J. M. Leger, P. Guionneau, I. Huc, *Org. Lett.* **2004**, *6*, 2985; g) J. K. H. Hui, M. J. MacLachlan, *Chem. Commun.* **2006**, 2480; h) J. S. Ferguson, K. Yamato, R. Liu, L. He, X. C. Zeng, B. Gong, *Angew. Chem.* **2009**, *121*, 3196; *Angew. Chem. Int. Ed.* **2009**, *48*, 3150; i) A. Filarowski, A. Koll, L. Sobczyk, *Curr. Org. Chem.* **2009**, *13*, 172; j) F. Li, Q. Gan, L. Xue, Z.-M. Wang, H. Jiang, *Tetrahedron Lett.* **2009**, *50*, 2367; k) B. Qin, W. Q. Ong, R. J. Ye, Z. Y. Du, X. Y. Chen, Y. Yan, K. Zhang, H. B. Su, H. Q. Zeng, *Chem. Commun.* **2011**, *47*, 5419; l) B. Qin, C. Sun, Y. Liu, J. Shen, R. J. Ye, J. Zhu, X.-F. Duan, H. Q. Zeng, *Org. Lett.* **2011**, DOI: 10.1021/ol200538d.

[5] a) Y. Y. Zhu, C. Li, G. Y. Li, X. K. Jiang, Z. T. Li, *J. Org. Chem.* **2008**, *73*, 1745; b) A. R. Sanford, L. Yuan, W. Feng, K. Yamato, R. A. Flowersb, B. Gong, *Chem. Commun.* **2005**, 4720; c) A. J. Helsel, A. L. Brown, K. Yamato, W. Feng, L. H. Yuan, A. J. Clements, S. V. Harding, G. Szabo, Z. F. Shao, B. Gong, *J. Am. Chem. Soc.* **2008**, *130*, 15784; d) P. S. Shirude, E. R. Gillies, S. Ladame, F. Godde, K. Shin-Ya, I. Huc, S. Balasubramanian, *J. Am. Chem. Soc.* **2007**, *129*, 11890; e) B. Qin, C. L. Ren, R. J. Ye, C. Sun, K. Chiad, X. Y. Chen, Z. Li, F. Xue, H. B. Su, G. A. Chass, H. Q. Zeng, *J. Am. Chem. Soc.* **2010**, *132*, 9564.

[6] a) B. Qin, X. Y. Chen, X. Fang, Y. Y. Shu, Y. K. Yip, Y. Yan, S. Y. Pan, W. Q. Ong, C. L. Ren, H. B. Su, H. Q. Zeng, *Org. Lett.* **2008**, *10*, 5127; b) Y. Yan, B. Qin, Y. Y. Shu, X. Y. Chen, Y. K. Yip, D. W. Zhang, H. B. Su, H. Q. Zeng, *Org. Lett.* **2009**, *11*, 1201; c) Y. Yan, B. Qin, C. L. Ren, X. Y. Chen, Y. K. Yip, R. J. Ye, D. W. Zhang, H. B. Su, H. Q. Zeng, *J. Am. Chem. Soc.* **2010**, *132*, 5869.

[7] a) Z. Zhang, B. Xia, C. Han, Y. Yu, F. Huang, *Org. Lett.* **2010**, *12*, 3285; b) C. Han, F. Ma, Z. Zhang, B. Xia, Y. Yu, F. Huang, *Org. Lett.* **2010**, *12*, 4360; c) Z. Zhang, Y. Luo, B. Xia, C. Han, Y. Yu, X. Chena, F. Huang, *Chem. Commun.* **2011**, 2417; d) Z. Zhang, Y. Luo, J. Chen, S. Dong, Y. Yu, Z. Ma, F. Huang, *Angew. Chem.* **2011**, *123*, 1433; *Angew. Chem. Int. Ed.* **2011**, *50*, 1397.

[8] a) Our examination of possible identities of the remaining compounds in the 50–60% reaction mixture produced from entries of Table 1 by TLC, MS, and ^{1}H NMR analysis only allows us to confidently conclude that it does contain small amounts of intermediate amino acids (e.g., dimer amino acid, trimer amino acid, and tetra amino acid) and does not contain any unreacted starting monomer amino acid, such as **1a**. Other than these compounds, the identity of other remaining compounds is unknown to us. b) From Table 1, entry 1, 8% of **1a** and 18% of **1b** was consumed in forming **3a** and **3b**, respectively. This left 92% of **1a** and 82% of **1b** participating in the two competition reactions that led to **3a** and **3b**. By assuming a simplified scenario, in which $K_{2+2}=K_{2+3}$ and a tetramer is generated from **1a** by a K_{2+2} reaction that leads to pentamer **3c**, the ratio of **3c** and **1** produced can be estimated to 1:1.9. Based on the 41% chemical yield for **1**, **3c** shall be produced in 24%. If the production of **3c** by the K_{2+3} reaction that involves dimer **1a** and in situ generated trimer is further considered, **3c** would be produced significantly more than 24%.

[9] a) Simulations were carried out by using a mechanism-based kinetics simulator from http://www.stolaf.edu/depts/chemistry/courses/toolkits/126/js/kinetics/index.htm; b) please note that the acyclic pentamer is unlikely to react with another monomer to form a circular hexamer, which is largely true experimentally. This assumption greatly reduces the complexity of kinetic simulations. See the Experimental Section for further descriptions.

[10] B. Gong, H. Q. Zeng, J. Zhu, L. H. Yuan, Y. H. Han, S. Z. Cheng, M. Furukawa, R. D. Parra, A. Y. Kovalevsky, J. L. Mills, E. Skrzypczak-Jankun, S. Martinovic, R. D. Smith, C. Zheng, T. Szyperski, X. C. Zeng, *Proc. Natl. Acad. Sci. USA* **2002**, *99*, 11583.

[11] S. Guieu, A. K. Crane, M. J. MacLachlan, *Chem. Commun.* **2011**, *47*, 1169.

[12] For full characterization data on **1**–**3**, see refs. [4k] and [4l].

[13] a) Gaussian 03, Revision C.02, M. J. Frisch et al., Gaussian, Inc., Wallingford CT, **2004**; b) A. D. Becke, *J. Chem. Phys.* **1993**, *98*, 5648; c) G. A. Petersson, A. Bennett, T. G. Tensfeldt, M. A. Al-Laham, W. A. Shirley, J. Mantzaris, *J. Chem. Phys.* **1988**, *89*, 2193; d) G. A. Petersson, M. A. Al-Laham, *J. Chem. Phys.* **1991**, *94*, 6081.

Received: April 25, 2011
Published online: July 20, 2011

